International Journal of Mechanical, Industrial and Aerospace Sciences
ISSN: 2517-9950
Vol:3, No:6, 2009

Tumble Flow Analysis in an Unfired Engine Using Particle Image Velocimetry

*B. Murali Krishna and J. M. Mallikarjuna

***Abstract*—**This paper deals with the experimental investigations of the in-cylinder tumble flows in an unfired internal combustion engine with a flat piston at the engine speeds ranging from 400 to 1000 rev/min., and also with the dome and dome-cavity pistons at an engine speed of 1000 rev/min., using particle image velocimetry. From the two-dimensional in-cylinder flow measurements, tumble flow analysis is carried out in the combustion space on a vertical plane passing through cylinder axis. To analyze the tumble flows, ensemble average velocity vectors are used and to characterize it, tumble ratio is estimated. From the results, generally, we have found that tumble ratio varies mainly with crank angle position. Also, at the end of compression stroke, average turbulent kinetic energy is more at higher engine speeds. We have also found that, at 330 crank angle position, flat piston shows an improvement of about 85 and 23% in tumble ratio, and about 24 and 2.5% in average turbulent kinetic energy compared to dome and dome-cavity pistons respectively.

***Keywords*—**In-cylinder flow, Dome piston, Cavity, Tumble, PIV

I. INTRODUCTION

NOW-A-DAYS, the modern lean-burn stratified and direct injection spark ignition (SI) internal combustion (IC) engines are becoming more popular because of their low fuel consumption and exhaust emissions. But, they have the problem of formation and control of the charge. This in turn affects the engine stability which is mainly dependent on the in-cylinder fluid flow structures. A practical approach to improve the engine stability with the lean mixtures is to shorten the combustion duration. This can be achieved by enhancing the tumble motion within the engine cylinder, which enhances the mean flow and turbulence of the mixture. Generating a significant vortex flows inside the IC engine cylinder during the intake process generates high turbulence intensity during the later stages of compression stroke leading to fast burning rates [1]. Now-a-days, in-cylinder flows are analyzed accurately using optical tool like particle image velocimetry (PIV).

Reference [2] carried out in-cylinder flow measurements using particle tracking velocimetry (PTV) and reported that the swirl and tumble flows should be maximized in order to maximize the turbulence for achieving good combustion. Reference [3] compared the effect on the tumble flow fields using different configurations of the pistons in a four-valve engine and found that, during the intake stroke, the vortex center lies initially under the intake valve/s and moved towards the exhaust valve/s later during the compression stroke. The laser doppler anemometry (LDV) measurements of the in-cylinder flows confirmed that the correlation between stronger tumble during induction and higher convective velocity, and turbulence levels near the spark gap at the time of ignition resulted in faster and stable combustion under lean mixture conditions [4].

Previous work clearly depicts that the in-cylinder flows have predominant effect on the engine performance and emission characteristics. Therefore, a good understanding of the in-cylinder flows in an IC engine is very much essential for the optimization of the engine parameters. The present experimental study involves two cases of in-cylinder tumble flow analysis on a vertical plane passing through axis of a single-cylinder, two-valve, unfired IC engine at various crank angle degrees (CADs) during suction and compression strokes using PIV. The first case deals with the in-cylinder tumble flows study using flat piston at the engine speeds of 400, 600, 800 and 1000 rev/min., and the second case uses dome and dome-cavity pistons at an engine speed of 1000 rev/min.

II. EXPERIMENTAL SETUP AND PROCEDURE

Figure 1 shows the photographic view of a single-cylinder, vertical, two-valve, air-cooled engine coupled to an induction motor of 5 hp through an electronic speed controller. The specifications of the engine are given in the Table.1. To facilitate the PIV measurements, an extended cylinder liner made of plexiglass and the corresponding extended piston are used at a compression ratio of 10. By this way, a field of view (FOV) of 87.5x35 mm is possible. The intake manifold of the engine is connected to a plenum to supply air and seeding particles uniformly.

The PIV system consists of a double pulsed ND-YAG laser with 200 mJ/pulse energy at 532 nm wave length, a charge coupled device (CCD) camera of resolution 2048x2048 pixels with a frame rate of 14 per second and a set of laser and camera controllers, and a data acquisition system and a software. The triggering signals for the laser and camera are generated by a crank angle encoder mounted on the engine

Authors are thankful to The Department of Science Technology (DST), Govt. of India, for sponsoring this project.

*B. Murali Krishna is with Internal Combustion Engine Laboratory, Department of Mechanical Engineering, Indian Institute of Technology Madras, Chennai - 600036, India (murali2kindia@gmail.com).

J. M. Mallikarjuna is with Internal Combustion Engine Laboratory, Department of Mechanical Engineering, Indian Institute of Technology Madras, Chennai - 600036, India

crank shaft with a resolution of one CAD are supplied to the controllers via a signal modulator. A master signal of the crank angle encoder is set to occur at the suction top dead center (TDC) of the engine (considered as a zero CAD). A seeding unit is used to generate the fine particles of one micron size with di-ethyl-hexyl-sebacat ($C_{26}H_{50}O_4$) as a seeding material. The laser sheet of 0.5 mm thickness is aligned with and camera is placed to view the FOV which is set on a vertical plane passing through the cylinder axis (Fig.2). Figure 3 shows the flat, dome and dome-cavity pistons used in this study along with the notations used to represent them.

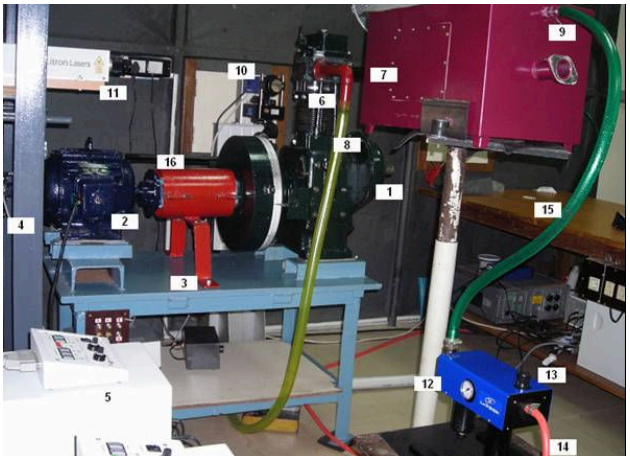

1. Engine
2. Motor
3. Test bench
4. Encoder
5. Laser controller
6. Transparent cylinder
7. Intake plenum
8. Exhaust
9. Air intake
10. CCD Camera
11. Laser
12. Seeder
13. Regulator
14. Compressor connection
15. Seeding supply
16. Coupling

Fig. 1. Photographic view of experimental setup

Table I. Engine specifications

Bore x stroke (mm)	87.5 x 110
Compression ratio	10:1
Rated engine speed (rrev/min.,)	1500
Maximum valve lift (mm)	7.6
Intake/exhaust port diameter (mm)	28.5
Intake valve opening (CAD bTDC)	4.5
Intake valve closing (CAD aBDC)	35
Exhaust valve opening (CAD bBDC)	35
Exhaust valve closing (CAD aTDC)	4.5

In this study, for both the cases, in-cylinder flow measurements are done during suction (30 to 180 CADs) and compression (210 to 330 CADs) strokes in steps of 30 CAD. At every measuring point, 500 image pairs are recorded and stored. The time interval (Δt) between the two images of a image pair is set based on the pixel shift (5 pixels), FOV, maximum expected velocity of fluid in FOV and resolution of camera [5 and 6]. To minimize the light reflections, a band-pass filter with central wavelength of 532 nm is mounted on CCD camera. LaVision DAVIS (data acquisition and visualization software) is used for image acquisition and data post-processing. During post-processing, interrogation window size of 32x32 pixels with multi-pass cross-correlation algorithm is used [7].

The ensemble average velocity vector fields are computed from the raw image pairs. Using them, tumble ratio (TR) and average turbulent kinetic energy (ATKE) are calculated at required CAD. For every setting, before taking the PIV measurements, the calibration of the in-cylinder environment as a whole is carried out along with plexiglass liner. The calibration procedure is repeated until a calibration root mean square (rms) fit error is less than 1.5 [5]. During the experiments, it is also ensured that clear images are captured every time. A typical raw image captured by PIV system at 30 CAD for the flat piston is as shown in the Fig.4.

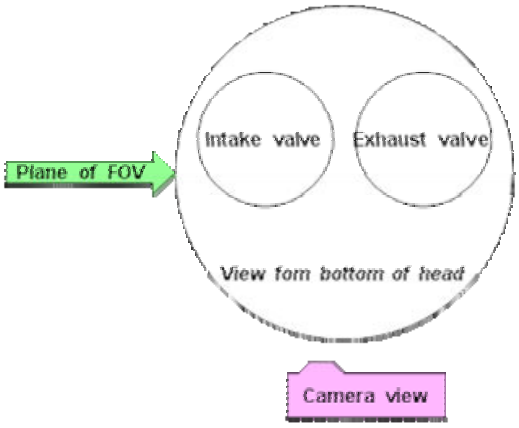

Fig. 2. Location of vertical plane passing through the axis of cylinder

Flat piston (F) | Dome piston (D) | Dome-cavity piston (D_b)

Fig. 3. Various piston crown shapes used

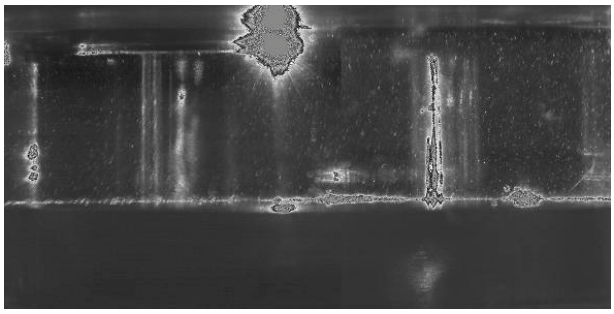

Fig. 4. Typical raw image of flat piston at 330 CAD

III. RESULTS AND DISCUSSION

In the following discussion, the ensemble average velocity vectors of the in-cylinder tumble flows are shown along with superimposed streamline patterns for better clarity. In these velocity vectors plots, constant length of velocity vector is used for all the vectors with a color bar to represent their magnitude. Each of these figures has their own colour bar to represent the velocity magnitudes.

Here, for flat piston, the ensemble average velocity vector fields during suction and compression stroke at an engine speed of 1000 rev/min., are only shown, since the in-cylinder flow patterns at the other engine speeds considered are almost similar to that of 1000 rev/min. Also, for dome and dome-cavity pistons, the tumble flow patterns are shown only during compression stroke at an engine speed of 1000 rev/min.

A. Tumble Flow Patterns during Suction Stroke

Fig.5 shows the ensemble average velocity vector fields during suction stroke for a flat piston at an engine speed of 1000 rev/min. In this case, at 30 CAD (Fig.5(a)), opening of the intake valve is about 15%. Also, at the left side of the intake valve, there is a very narrow passage for the air to enter the cylinder space causing minimum air entry at this side. Therefore, more amount of air flows at right side of the intake valve. The air enters the cylinder at the right side in the form of a jet almost parallel to the cylinder head. Air jet reaches the right side cylinder wall, strikes it, diverted downwards and again strikes piston top surface, forming a clockwise (CW) vortex. In the similar manner, small amount of air entering the cylinder space at the left side of the intake valve, forms a counter clock wise (CCW) vortex. Since, the air flow at the top of the combustion chamber is more predominant and also inlet valve acts as a bluff body, central cylinder space becomes a low pressure zone. Therefore, some amount of air from the other regions of the cylinder space rush towards the low pressure zone and mixes with the ambient air very rapidly. At 60 CAD (Fig.5(b)), inlet valve has opened by about 60%. At this condition, air flows at right side of the inlet valve bending downwards and moving rightwards in the form of a jet. Due to downward bending of the air jet, some amount of air is forcing to the cylinder space at top right corner of FOV and major part of the air moves rightwards. Due to comparatively large opening of inlet valve, air flow rate increases and also due to more cylinder space above the piston top, a large CW vortex forms at right side cylinder space as explained above. Because of the flow diversification at the right side cylinder space, there exists a flow bifurcation zone seen as a thick stream line in Fig.5(b). At the left side, in the similar way, a large CCW vortex forms. At the center space just below the intake valve, due to the collision of the CW and CCW vortices, another bifurcation zone is created.

At 90 CAD (Fig.5(c)), the intake valve opens for about 90% (full opening at 110 CAD) and also the piston speed reaches the peak and therefore air flow rate is maximum at this condition. At this CAD, air jet at the right side of the intake valve moves with full velocity almost parallel to the cylinder axis. A part of the air flows towards left side, strikes the piston top surface and diverting upwards left forming a large CW vortex. Other part of the air flows to right side, after striking the piston top surface, moves further right and striking the right cylinder wall moving right upwards and forms a large CCW vortex. The formation of the two large vortices is also assisted by the low pressure regions just below the intake valve and at the right side cylinder space. From Fig.5(c), it is very much clear that at the right side cylinder space below the intake valve, due to the flow diversification, a clearly visible bifurcation zone is created. The air flow at the left side of the intake valve, after striking the left cylinder wall is entering the left side cylinder space below the intake valve. However, due to the dominant right side air flow, an almost vertical bifurcation zone is created very close to the left cylinder wall. At 120 CAD (almost full intake valve lift, Fig.5(d)), the tumble flow pattern is almost similar to that of 90 CAD. However, at this CAD, size of the vortices increase and it may be due to the expansion of the fluid because of downward movement of piston. At 150 CAD (Fig.5(e)) also, the in-cylinder flow pattern is similar to that of 120 CAD; however, the size of two vortices to the right side of the intake valve is shrinking. This may be due to reduction of the air flow rate by the closer of the intake valve and further expansion of the air at this CAD. In addition, a dominant CCW vortex at left side cylinder space just below the intake valve is created.

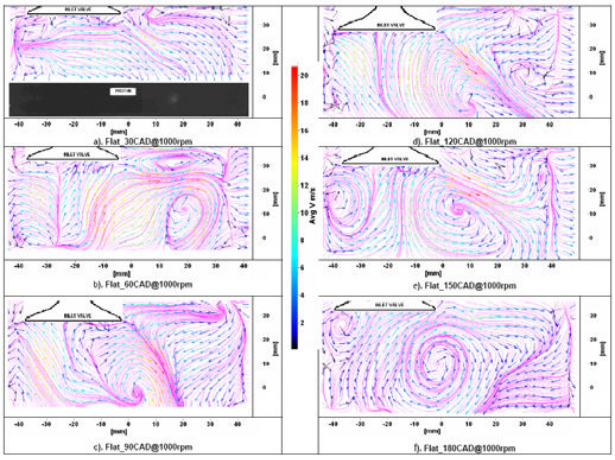

Fig. 5. Ensemble average velocity vectors of flat piston during suction stroke at 1000 rev/min.

At 180 CAD (Fig.5(f)), intake valve opening is very less, hence fresh air entry is also less. However, the air which is already present during the early part of the cycle is under going the changes. From Fig.5(f), it can be observed that, a large CW vortex forms almost dominating the entire cylinder space with center lying below the intake valve. Also, From Fig.5(f), it can be observed that the formation of a small vortex near the left top corner of the FOV. This may be due to the low pressure region at that point because of a large vortex

formation at the central cylinder space.

The in-cylinder tumble flow ensemble average velocity vectors for the dome and dome-cavity pistons during suction stroke at corresponding CADs are almost similar to that of flat piston, except the variation in the vector magnitudes. A better comparison of the tumble flow patterns with these piston crown shapes is made later with the help of tumble ratio (TR) and average turbulent kinetic energy (ATKE). Here, the intention of adding the cavity to dome piston is to assist and retain the tumble vortex along the axis of the cylinder, where the spark plug and fuel injectors would be fitted in the combustion chamber in direct injection SI engines.

B. Tumble Flow Patterns during Compression Stroke

Fig.6 shows the in-cylinder tumble flow patterns for a flat piston during the compression stroke on a central vertical plane at an engine speed of 1000 rev/min. At 210 CAD (Fig.6(a)), a large single CW vortex created at the end of suction stroke shifts towards left side of the cylinder with reduction in size. In addition, air flow from the other zones of the cylinder space after striking the right cylinder wall, tries to form a CCW vortex near the right cylinder wall. Both the vortices strike each other and form a bifurcation zone near the right side cylinder space. This may be also due to the upward motion of the piston during compression stroke which squeezes entire in-cylinder flow pattern as a whole. At 240 CAD (Fig.6(b)), there are no much changes in the in-cylinder flow patterns compared to 210 CAD, except the increase in size of single large vortex. Also, bifurcation zone created earlier is tries to move leftwards.

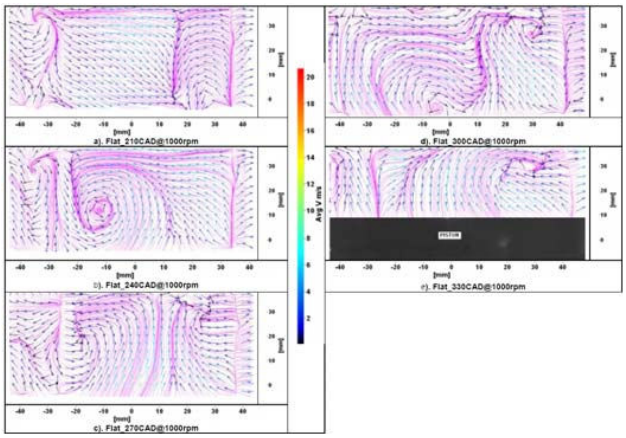

Fig. 6. Ensemble average velocity vectors of flat piston during compression stroke at 1000 rev/min.

At 270 CAD (Fig.6(c)), in-cylinder flow pattern is divided almost into three clear zones. At the cylinder space near the right and left cylinder walls, two CCW vortices form and at the center space, a CW vortex has been formed. This may be due to the striking of the vertically upward air flow with the cylinder head caused by the upward movement of the piston and also due to the reduction in cylinder space. Additionally, it may be due to the air flow rushing into the low pressure zones at the center cylinder space from the other zones.

At 300 CAD (Fig.6(d)), piston moves further up and thereby reducing the cylinder space. Therefore, the large vortices formed earlier vanish. From Fig.6(d), it is seen that, the entire air flows upward almost maintaining the two bifurcation zones created earlier. Also, small vortices are created at right side cylinder space. It may due to higher velocities of the CW vortex. Fig.6(e) shows the in-cylinder flow pattern at 330 CAD, it is observed that there is a clear CW vortex formation almost at the top center of combustion space. Normally, in the stratified charge and direct injection SI engines, spark plug is located at the center of combustion chamber. Therefore, once ignition starts, the air movement and the vortex formation inside the combustion space would aid proper flame propagation resulting in effective combustion. Formation of vortex and CW air movement is almost evident at all engine speeds.

Fig.7 shows the in-cylinder tumble flow patterns for dome piston during the compression stroke. At all the CADs considered, the tumble flow patterns are similar to those of flat piston at the corresponding CADs, except the variation of velocity vector magnitudes. Also, randomness in in-cylinder tumble flow pattern is observed at 330 CAD with this type of piston crown shape. In this case, the in-cylinder tumble flow pattern is more dominated by CCW movement of air unlike the case of flat piston. At 300 CAD, piston moves further up and thereby cylinder space has further reduced. Therefore, size of the vortices formed earlier reduces. From Fig.7(d), it is seen that the entire cylinder air moves upwards and also towards right side causing CW flow. From Fig.7(e), it is observed that, at 330 CAD, the bifurcation zones still exists and no clear vortex formation is seen in the combustion space, however the tumble flow pattern looks more random compared to that of flat piston.

Fig.8 shows the in-cylinder tumble flow patterns for dome-cavity piston during the compression stroke. In this case, the tumble flow patterns are similar to those of dome piston at the corresponding CADs. From Fig.8(e), it is observed that the tumble flow patterns look more organized than those of dome piston.

It is very much clear that irrespective of the formation of vortex and air flow movement at earlier stages of the cycle, a favorable air flow pattern needs to occur at 330 CAD which is very much useful especially for the stratified charge and direct injection SI engines. The air movement at this crank angle position plays a very vital role in ignition and flame propagation. Higher the turbulence during compression is believed to generate both faster flame propagation and higher reactive flame-surface area [2]. In general, the magnitudes of velocity vectors are reducing during compression stroke irrespective of the piston crown shapes considered and size of the tumble vortex increases towards the end of suction stroke. Also, the vortex center moves generally towards the exhaust valve side during compression. However, the effect of the piston crown shape on the in-cylinder tumble flows can be

better understood with the help of tumble ratio (TR) and average turbulent kinetic energy (ATKE) of the flow as follows.

C. Variation of Tumble Ratio

The overall in-cylinder air movement is difficult to quantify just by a visual inspection of the velocity vector fields. However, it can be done with the help of TR. Unlike swirl ratio which usually obtained through steady flow experiments, tumble ratio must be evaluated under transient conditions due to significant effect of the piston crown shape and its motion on the in-cylinder tumble flows [2]. In this study, in-cylinder tumble flow is characterized by TR calculated from an equation proposed by Huang et al., [8]. The negative or positive magnitudes of TR indicate the direction of the overall in-cylinder tumble flows at a given plane as CW or CCW respectively.

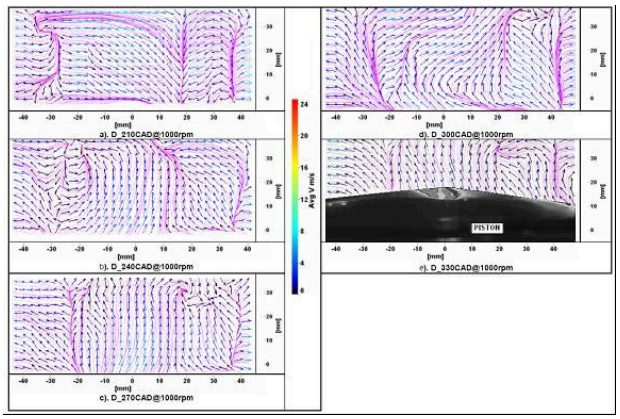

Fig. 7. The ensemble average velocity vectors of dome piston during compression stroke at 1000 rev/min.

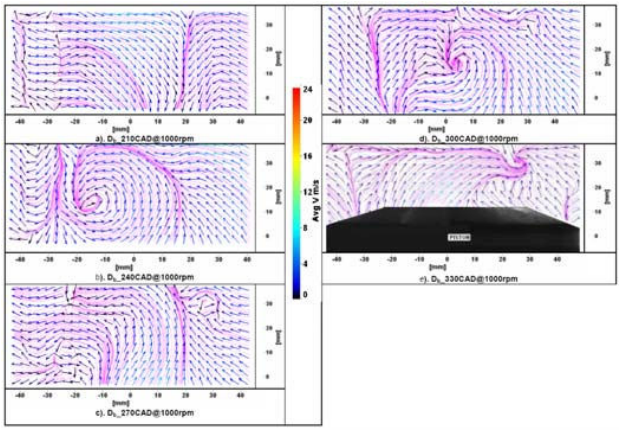

Fig. 8. The ensemble average velocity vectors of dome-cavity piston during compression stroke at 1000 rev/min.

Fig.9 shows the variation of the TR with CADs at various engine speeds considered in this study during suction and compression strokes. From Fig.9, it is observed that the TR ratio changes its magnitude (positive to negative or vice versa) indicating overall air movement changes its direction during entire cycle with CADs. The reasons for this could be: (i) change in the overall tumble flow pattern due to low pressure and bifurcation zones, (ii) change in piston speed with CADs, and (iii) change in the direction of the piston movement during suction and compression strokes. With an increase in engine speed, variation in TR is marginal at all the CADs. However, at 330 CAD, TR is maximum at higher engine speed.

Fig.10 shows variation of TR at different CADs during suction and compression at an engine speed of 1000 rev/min., for three piston crown shapes considered in this study. From Fig.10, it is observed that variation of TR with CADs is similar for all the piston crown shapes considered. But, the magnitudes vary with type of piston. Stronger the tumble motion (more TR), more the turbulent kinetic energy released during its break down at the end of compression stroke. Also, it helps in higher turbulence levels at the time of ignition. Among the piston crown shapes considered in this study, flat piston results in higher TR compared to the dome and dome-cavity pistons.

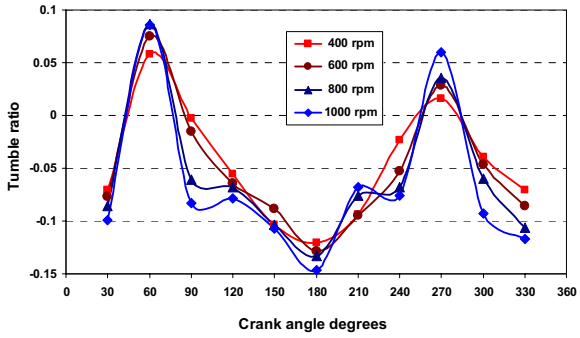

Fig. 9. Variation of TR with crank angle positions for a flat piston at various engine speeds

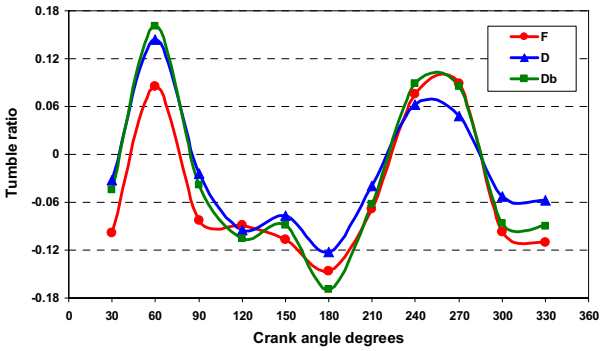

Fig. 10. Variation of TR with crank angle positions for different piston crown shapes at 1000 rev/min

Flat piston shows an improvement of about 85 and 23% in TR compared to the dome and dome-cavity pistons respectively. Tumble flow is more effective than swirl for efficient dissipation of the inertia and kinetic energy of piston

into turbulence at the end of compression stroke.

D. Variation of Turbulent Kinetic Energy

Turbulent kinetic energy of flow indicates its strength as a whole. Fig.11 shows variation of average turbulent kinetic energy (ATKE) with CADs during suction and compression strokes at different engine speeds. From Fig.11, it can be observed that, ATKE is more at higher engine speeds indicating higher strength of the flows.

Fig.12 shows variation of ATKE at various CADs during suction and compression strokes for different piston crown shapes considered. From Fig.12, the magnitudes of ATKE are peaking at 60 CAD. It may be due to higher velocity of the incoming air, because at this CAD, piston moves with higher velocity, it has moved sufficiently down and also inlet valve is sufficiently open. Afterwards, ATKE drops gradually upto 180 CAD and then remains almost constant until the end of the compression stroke. Profile of the ATKE with crank angle positions obtained in this study is similar to that of [9]. From Fig.12, it is evident that ATKE is higher for dome-cavity piston compared to dome piston. However, flat piston is the best compared to other two pistons considered. At 330 CAD, flat piston shows an improvement of about 24 and 2.5% in ATKE compared to dome and dome-cavity pistons respectively.

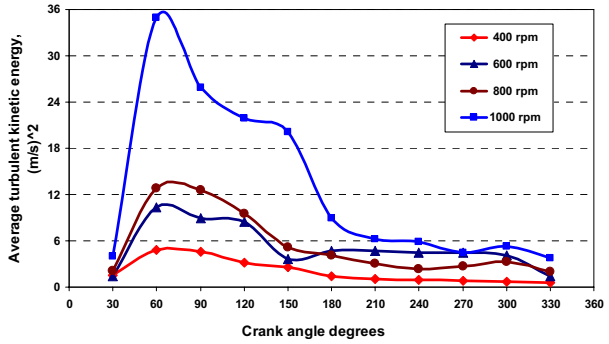

Fig. 11. Variation of ATKE with crank angle positions for a flat piston at various engine speeds

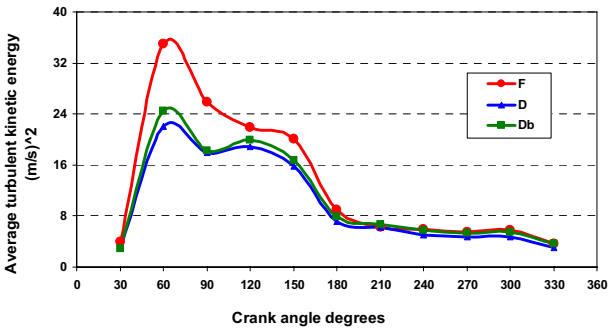

Fig. 12. Variation of ATKE with crank angle positions for different piston crown shapes at 1000 rev/min

IV. Conclusions

From the experimental study of the tumble flows in a single-cylinder, two-valve, IC engine using different piston crown shapes under unfired conditions using PIV, the following conclusions are drawn:

The overall in-cylinder tumble flows are much dependent on the crank angle positions irrespective of engine speed.

At the end of compression stroke, where spark is supposed to be supplied, ATKE is higher at higher engine speeds.

At 330 CAD, flat piston top shows an improvement of about 85 and 23% in tumble ratio compared to dome and dome-cavity pistons respectively.

At 330 CAD, flat piston top shows an improvement of about 24 and 2.5% in average turbulent kinetic energy compared to dome and dome-cavity pistons respectively.

It is suggested to use the flat piston rather than dome, dome-cavity pistons which are rather difficult to manufacture as far as tumble flows are concerned.

Acknowledgments

The authors are thankful to the staff members: Mr. K. Nagarajan, Mr. M. K. Subramanian, Mr. M. Michael John Bose and Mr. S. Babu of IC engines Laboratory, Indian Institute of Technology Madras, Chennai, India for assisting in carrying out the experiments.

References

[1] J. B. Heywood (1988), Internal Combustion Engine Fundamentals, Pub: McGraw Hill International Editions.
[2] B. Khalighi (1991), Study of the Intake Tumble Motion by Flow Visualization and Particle Tracking Velocimetry, Journal of Experiments in Fluids, Vol 10, pp.230 236.
[3] B. Xavier and F. Alain (1997), Investigation of the In-Cylinder Tumble Motion In a Multi Valve Engine: Effect of Piston Shape, Paper No. SAE 971643.
[4] C. Arcoumanis, C. S. Bae, and Z. Hu, Flow and Combustion in a Four-Valve, Spark-Ignition Optical Engine, Paper No. SAE 940475
[5] DAVIS 7.2: *Software Manuals*, LaVision, Germany, 2006.
[6] B. Murali Krishna and J. M. Mallikarjuna, "Optical Diagnosis of Flow through the Intake Valve in a Direct Injection Diesel Engine", *Proceedings of the 15Th ISME International Conference on New Horizons of Mechanical Engineering (ISME-2008)*, March 18-20, Bhopal, India, 2008.
[7] M. Raffel, C. Willet and J. Kompenhans, *Particle Image Velocimetry-A Practical Guide*, Pub: Springer-Verlag Berlin Heidelberg, Germany, 1998.
[8] R.F. Huang, C.W. Huang, S.B. Chang, H.S. Yang, T.W. Lin, W.Y. Hsu, "Topological Flow Evolutions In-cylinder of A Motored Engine During Intake and Compression Stroke", *Journal of Fluids and Structures*, Vol 20, pp.105–127, 2005.
[9] Y. Li, H. Zhao and T. Ma, "Flow and Mixture Optimization for a Fuel Stratification Engine using PIV and PLIF Techniques", *Journal of Physics: Conference Series*, Vol 45, pp 59–68, 2006.